



PERGAMON

Scripta mater. 43 (2000) 515–521



www.elsevier.com/locate/scriptamat

## CRUSHING OF ALUMINUM CLOSED CELL FOAMS: DENSITY AND STRAIN RATE EFFECTS

I.W. Hall, M. Guden\* and C.-J. Yu<sup>†</sup>

Department of Mechanical Engineering, University of Delaware, Newark, DE 19716 \*Izmir Yuksek Teknoloji Enstitüsü, Izmir, Turkey <sup>†</sup>Fraunhofer Center-Delaware, 501 Wyoming Road, Newark, DE 19716

(Received October 1, 1999)

(Accepted in revised form April 11, 2000)

### Introduction

Potential applications of metal foams include light weight cores for sandwich panels, shells and tubes where the foam can increase the resistance to local buckling, increase the impact resistance, and improve the energy absorbing capacity of the structure [1,2]. This latter property offers potential uses in transportation applications where, for example, foam-filling of the hollow sections of automobiles, such as fenders, may reduce damage and injuries resulting from impact accidents. For this type of application, aluminum foam is more suitable than a polymeric foam, because it deforms plastically under impact and with essentially no spring back, preventing further damage [3]. Other important advantages of using aluminum foams over polymeric foams include high fire resistance and insensitivity to cold and hot weather and humidity [3].

Impact accidents produce loading rates which are higher than those of static or quasi-static rates and which may significantly alter mechanical response of the materials. Therefore, in designing with metallic foams as energy absorbing fillers, mechanical properties are needed for strain rates corresponding to those created by impact events. Quasi-static mechanical behavior of metallic foams has been fairly extensively studied and reported, e.g. [3–5], but data concerning high strain rate mechanical behavior of these materials are, however, only just becoming available and are rather sparse [6,7]. This study was initiated, therefore, to study the high strain rate mechanical behavior of a range of metallic foams, and to compare it with quasi-static behavior and, hence, determine any effect on energy absorbing capacity. Microscopic observations were also made in order to clarify the deformation mechanisms involved during crushing of the foam.

### Material and Testing Methods

The metal foam investigated in this study was manufactured by the Fraunhofer Center - Delaware, using a patented powder metallurgical technique [8]. One of the advantages of this method is that it is possible to manufacture complex structures to near net shapes. The foam was prepared using 6061-Al alloy powder and TiH<sub>2</sub> as the foaming agent and was supplied as rectangular plate (50 mm thick and 100 mm wide) with a typical closed cell structure. The cell size varied somewhat through the thickness and

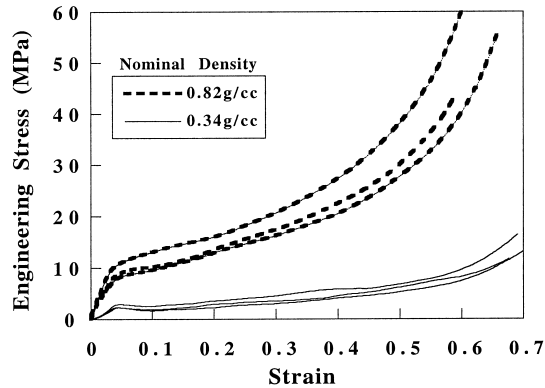


Figure 1. Quasi-static eng. stress vs. eng. strain curves for samples of two different nominal densities.

resulted, therefore, in a slight density gradient. Typical cell sizes were 4–5mm in the mid-sections and 2–3mm near to the external surfaces.

Quasi-static compression tests were conducted using a displacement controlled Instron machine at an initial strain rate of  $1.5 \times 10^{-3} \text{ s}^{-1}$ . High strain rate tests were conducted using a compression-type Split Hopkinson Pressure Bar (SHPB), also known as a Kolsky Bar. Briefly, in this technique a cylindrical specimen is mounted between the long incident and transmitter bars, while a shorter striker bar is used to impact the end of the incident bar. This impact creates a compressive pulse which travels down the incident bar and into the specimen which then deforms as it is sandwiched between incident and transmitter bars.

Conventionally, the strains measured by strain gages on the incident and transmitter bars are then used to determine strain rate, strain and stress in the specimen using one dimensional elastic wave analysis [9]. However, tests on foams violate several of the fundamental assumptions of this type of analysis: for example, the volume does not remain constant during testing and the elastic wave velocity depends on the density which itself changes during the test. Nevertheless, and bearing in mind that these are non-standard tests with limitations, it is found that conventionally-reduced SHPB foam data resemble the stress-strain curves which would be anticipated from quasi-static tests. Consequently, and also since an acceptable alternative means of data presentation has not yet been developed, the data are presented as engineering stress vs. engineering strain curves.

High strain rate tests were conducted on the foam at strain rates up to  $\sim 2.0 \times 10^3 \text{ s}^{-1}$ . The strain rates involved in automobiles during impact accidents are most frequently in the range between  $\sim 1 \times 10^2$  and  $\sim 1 \times 10^3 \text{ s}^{-1}$  and the investigated strain rates are, therefore, relevant to impacts involved in such accidents.

The cylindrical foam specimens were 18mm in diameter and 12mm tall. Some scatter was observed in the data (see Fig. 1 below) but was not reduced by the use of larger samples. The diameter of the samples was slightly less than that of the bars (19mm) and, due to the small Poisson's ratio of the foam, specimen diameters during deformation never exceeded the bar diameter within the studied strain levels up to  $\sim 60\%$  strain. The relatively large diameter of the SHPB used was advantageous, since larger volumes of foam could be tested, thus reducing statistical scatter somewhat. By conducting tests on identically sized specimens in the Instron, any significant effect of specimen volume on the measured flow stress was avoided.

Flow stresses reported below were determined at 10% strain since a) severe initial stress drops were noted in many of the tests and b) an inherent feature of the SHPB apparatus is that flow stress values

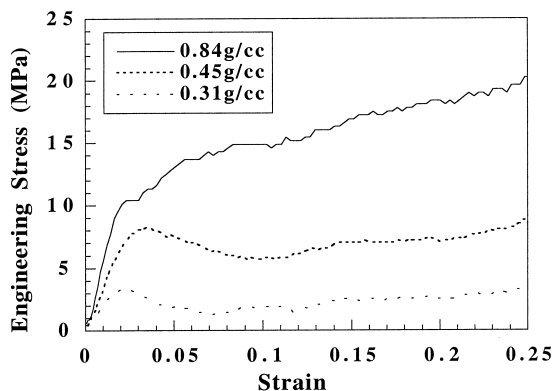


Figure 2. Stress vs. strain curves at  $2 \times 10^3 \text{ s}^{-1}$  for samples of three different (individually measured) densities.

at small strains, such as the yield strain, can not be determined due to the absence of stress equilibrium in the early stages of the test.

Foam blocks with average densities of 0.34, 0.47, 0.57 and  $0.82 \text{ gcm}^{-3}$  were used. Specimens were core-drilled through the thickness direction of the foam blocks and then individually weighed and measured in order to calculate the actual and relative densities before testing. The relative density,  $\rho^*$ , is calculated as:

$$\rho^* = \frac{\rho_f}{\rho_m} \times 100\% \quad (1)$$

where f and m refer to the foam and precursor (matrix) alloy respectively. The average relative densities of the four foam blocks were, therefore, 12.6%, 17.4%, 21.1% and 30.4% respectively.

## Results

Typical quasi-static compressive engineering stress-strain curves from 3 samples of each of the lowest and highest density foams are shown in Fig. 1. It is seen that the flow stress is a strong function of relative density and the curves show the typical shape which may be divided into three regions, 1) linear elastic region, 2) collapse region and finally, 3) a densification region in which the properties approach those of fully-dense alloy. It is also seen that, for the low density foams, a load drop occurs after the initial elastic extension while the higher density ones exhibited no load drop. Also, stress oscillations occur in the collapse region of low density samples while the higher density ones showed an essentially monotonic increase in stress throughout the tests. The flow stress in the collapse region increased as the relative density increased, as expected, but the rate of densification was also higher in the denser samples. Strains in excess of 60% were easily achieved in all cases.

Foams were then tested in the SHPB and Fig. 2 shows typical stress-strain curves for foams of three different densities tested at  $2 \times 10^3 \text{ s}^{-1}$ . Again, the flow stress values of the foam are seen to be a strong function of relative density although it is also noted that the areas under the stress strain curves, which scale with the energy absorbed, do not scale linearly with the density. The respective areas under the curves were calculated between 5% and 25% strain, the latter being the maximum strain obtainable at the lowest strain rate in the SHPB, and the data are plotted as a function of density in Fig. 3. Fig. 4 shows data for foams, with individually measured densities of  $0.52 \text{ gcm}^{-3}$ , tested over a range of strain rates from quasi-static to  $2 \times 10^3 \text{ s}^{-1}$  and up to  $\sim 25\%$  strain. Even when minor variations in density

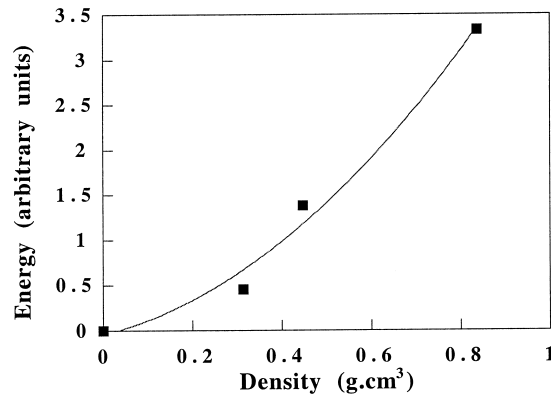


Figure 3. Energy absorbed as a function of density, between 5, and 25% strain.

are removed, there is still no unequivocal effect of strain rate within this strain range and the areas under the curves, were approximately equal. The absence of marked strain rate sensitivity is in agreement with other observations for this and other aluminum alloys [10,11].

The sequence of deformation events was recorded during quasi-static compression testing and several frames of a typical record are presented in Fig. 5. The time at each frame is marked and the compression loading axis was horizontal. Frame 1, 0s, shows an undeformed region containing several cells. As soon as compression starts the thinnest sections of cell walls approximately parallel to the compression axis start to buckle, 20s. In the later stages of deformation, frames at 90s and 120s, cell walls normal to the compression axis tear due to the induced tensile strains. It may also be noted that deformation is highly inhomogeneous and that cells to the left are completely undeformed while adjacent ones are almost totally closed up.

Microscopic examination of cell walls showed clear evidence of the original powder particles, Fig. 6; the walls were made up of many particles sintered together confirming that complete melting had not occurred. These surfaces also exhibited particles which were identified by EDS measurements as being rich in Ti (arrowed in Fig. 6). The cell walls were also coated with a thick ( $0.5\mu\text{m}$ ) layer of oxide and cross sections of the foam showed that cell boundaries were important during compression since, upon buckling or tearing of cell walls, fracture proceeded through these boundaries as shown in Fig. 7.

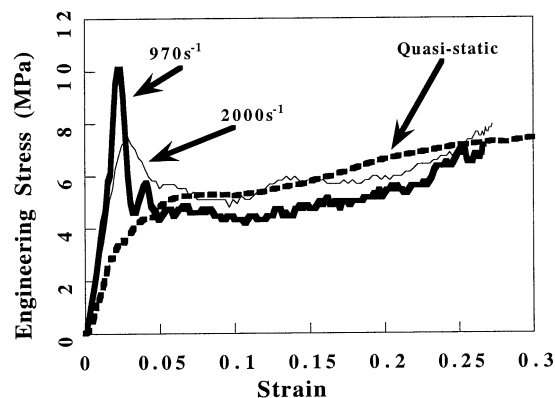


Figure 4. Typical eng. stress vs. strain curves for 3 samples with densities of  $0.52\text{gcm}^{-3}$ .

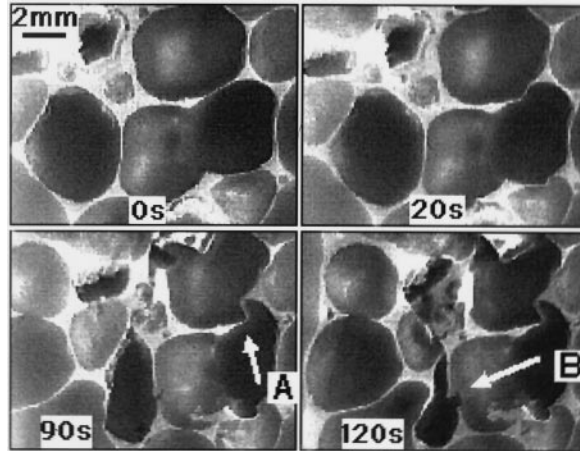


Figure 5. Time lapse sequence showing inhomogeneous deformation, buckling (A) and tensile tearing (B).

### Discussion

A general relationship relating the compressive strength mechanical properties of foams to their density,  $\rho$ , has been previously proposed as [12]

$$\frac{X_f}{X_s} \sim K(\rho^*)^n \quad (2)$$

where  $X$  is a property such as the modulus or engineering yield stress,  $f$  and  $s$  refer to foam and dense solid respectively, and  $K$  and  $n$  are constants (at fixed strain rate). Eq. 2 was developed for open cell foams and the following equation has been proposed for the yield strength of closed cell foams [5]

$$\frac{\sigma_f}{\sigma_s} = 0.3 (\phi \rho^*)^{3/2} + (1 - \phi) \rho^* \quad (3)$$

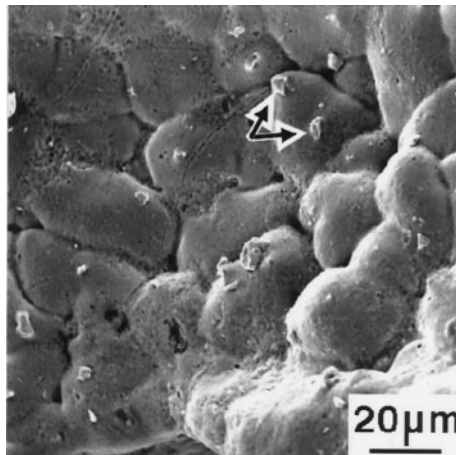


Figure 6. Interior surface of pore, showing evidence of prior powder particles and Ti-rich particles (arrowed).

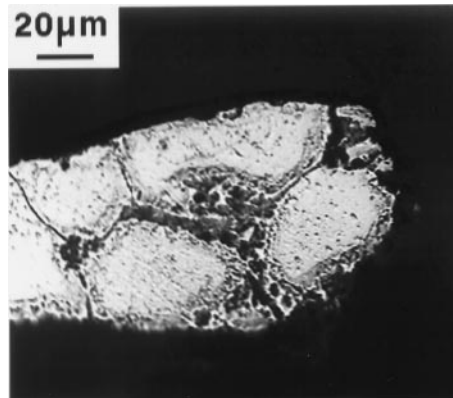


Figure 7. Section through broken cell wall, showing outlines of original powder particles.

where  $f$  is a measure of the distribution of solids between cell walls and edges. The first term in Eq. 3 is due to bending and the second is due to membrane stretching. It is noted that in both Eqs. 2 and 3, the foam's mechanical properties scale with the precursor alloy properties. Eq. 2 was also found to fit the experimental yield strength of closed cell foams quite well for the case of easily rupturing cell walls [3].

In order to determine the effect of strain rate on the flow stress of the foam, quasi-static and dynamic flow stresses were fitted to the power law equation (Eq. 2) for 4 different strain rates. It was found that Eq. 2 fits quasi-static and dynamic flow stresses well and that the value of  $n$  was apparently 1.9 for quasi-static and  $2. \times 10^3 \text{ s}^{-1}$  strain rates, while it was 2.4 for intermediate strain rates of  $3 \times 10^2 \text{ s}^{-1}$  and  $1 \times 10^3 \text{ s}^{-1}$ . Not only are these  $n$  values higher than previously reported values of approximately 1.5 [12], but they also show an apparently anomalous dependence on strain rate. However, it is considered that much of the variability reflects an inherent problem with measurements on foams, namely, the difficulty associated with obtaining uniform densities throughout a range of samples. Fig. 8, for example, shows all the data from the present tests, sorted by strain rate and presented as a function of density. It can be seen that there is no clear dependence of flow stress on strain rate although the power law fits the data well with an average exponent,  $n$ , of 2.1. Further work is underway to generate a larger database and to attempt to normalize the data with respect to density in order to determine whether there is a real effect of strain rate on flow stress.

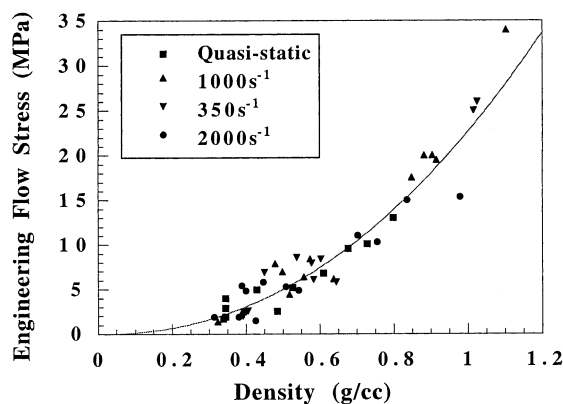


Figure 8. All data, for all strain rates, plotted as function of density.

Since, as mentioned above, one of the projected uses of such foams is for energy absorption (area under the stress/strain curve), it is clearly of interest to consider this property. In the present case it has also been found that, similarly to other mechanical properties, the relationship between energy absorption,  $U$ , and density closely fits an equation of the form of Eq. 2. Again,  $n$  was found to be  $\sim 1.9$ , higher than previously reported values but nevertheless scaling well with the increase in flow stress noted before.

An increase in flow stress with strain rate has been noted in polymeric closed cell foams [6] and the increase in flow stress, especially at high strain rates, is believed to be partly due to the inability of gas to escape from inside the cells and partly due to strain rate sensitivity of the polymers. In the case of metal foams, and in open cell polymeric foams, any strain rate dependence of the flow stress is principally due to the strain rate sensitivity of the matrix materials. In marked contrast to previous work [6], the present foam does not exhibit strain rate sensitivity, or at most only a very weak dependence which is masked by the scatter in experimental data. Further work is necessary to clarify the issue of strain rate sensitivity.

An important observation, therefore, is that foam properties are extremely sensitive to minor variations in density and that, either, future testing must be performed on sample numbers large enough to provide statistically meaningful data, or test data must be normalized with respect to density.

### Conclusions

Quasi-static and high strain rate compression behavior of an Al closed cell foam has been determined and the following can be concluded;

1. The compressive flow stress of the foam was a function of the relative density but exhibits little or no strain rate sensitivity.
2. It has been shown that, in addition to the flow stress, the energy absorption is also related to the foam density by a similar power law dependency.
3. Metallographic observations of compressively deformed foam confirmed the general processes of progressive cell wall collapse, including buckling and tearing modes, and also highlighted the role of precursor powder particle boundaries in these events.

### Acknowledgments

The authors gratefully acknowledge financial support from the U.S. Army Research Office (Drs. J. Bailey & D. Stepp, Program Monitors) and from Honda R&D Americas, Inc.

### References

1. M. Seitzburger, F. G. Rammerstorfer, H. P. Degischer, and R. Gradinger, *Acta Mech.* 125, 93 (1997).
2. C. L. Wu, C. A. Weeks, and C. T. Sun, *J. Advan. Mater.* 41 (1995).
3. J. T. Beals and M. S. Thompson, *J. Mater. Sci.* 32, 3595 (1997).
4. O. Prakash, H. Sang, and J. D. Embury, *Mater. Sci. Eng. A199*, 195 (1995).
5. Y. Sugimura, J. Meyer, M. Y. He, H. Bart-Smith, J. Grenstedt, and A. G. Evans, *Acta Mater.* 45, 5245 (1997).
6. T. Mukai, H. Kanahashi, T. Miyoshi, M. Mabuchi, T. G. Nieh, and K. Higashi, *Scripta Mater.* 40, 921 (1999).
7. F. Han, Z. Zhu, and J. Gao, *Met. Mat. Trans. A.* 29A, 2497 (1998).
8. C.-J. Yu, H. Eifert, J. Banhart, and J. Baumeister, *J. Mater. Res. Innov.* 2, 181 (1998).
9. M. Guden and I. W. Hall, *Mater. Sci. Eng. A242*, 141 (1998).
10. S. Yadav, D. R. Chichili, and K. T. Ramesh, *Acta Metall. Mater.* 43, 4453 (1994).
11. C. H. Maiden and S. V. Green, *ASME J. Appl. Mech.* 33, 496 (1966).
12. M. F. Ashby, A. G. Evans, J. W. Hutchinson, and R. A. Fleck, *Metal Foams: A Design Guide*, Ultralight Metal Structural Conference, Brewster, MA (1998).